33rd Annual International Conference of the IEEE EMBS
Boston, Massachusetts USA, August 30 - September 3, 2011

Upper Limb Joint Angle Tracking with Inertial Sensors

Mahmoud El-Gohary, Lars Holmstrom, Jessie Huisinga, Edward King, James McNames, and Fay Horak

Abstract— **Wearable inertial systems have recently been used to track human movement in and outside of the laboratory. Continuous monitoring of human movement can provide valuable information relevant to individual's level of physical activity and functional ability. Traditionally, orientation has been calculated by integrating the angular velocity from gyroscopes. However, a small drift in the measured velocity leads to large integration errors that grow with time. To compensate for that drift, complementary data from accelerometers are normally fused into the tracking systems using the Kalman or extended Kalman filter (EKF). In this study, we combine kinematic models designed for control of robotic arms with the unscented Kalman filter (UKF) to continuously estimate the angles of human shoulder and elbow using two wearable sensors. This methodology can easily be generalized to track other human joints. We validate the method with an optical motion tracking system and demonstrate correlation consistently greater than 0.9 between the two systems.**

I. Introduction

Measurement and analysis of human movement has many applications including assessment of neurological movement disorders, rehabilitation from injury, and enhancement of athletic performance. Movement can be measured using a wide variety of techniques and sensors. Wearable inertial sensors enjoy the advantages of being simple, unobtrusive, and self-contained. They are well suited to recording long-term monitoring while the subject performs normal activities of daily life at home. A typical wearable inertial sensor is a compact wearable device that contains a triaxial accelerometer and triaxial gyroscope. Fig. 1 shows an example of Opal sensor (APDM, Inc., Portland, OR) used in this study. Traditionally, the orientation of a body segment is estimated by integrating the angular velocity measured by gyroscopes, and position is obtained by double integration of the translational acceleration measured by accelerometers. A significant problem with integration, however, is that inaccuracies inherent in the measurements quickly accumulate in the integrated estimation, resulting in an unacceptable levels of position error in as little as 10–60 s [1]. Roetenberg showed that integration of gyroscope data resulted in a drift between $10 - 25^\circ$ after one minute [2]. One approach to reducing integration drift is to fuse the gyroscope data with complementary data from other sensors. Luinge *et al.* estimated orientation by fusing gyroscope and accelerometer data [3]. The difference between tilt computed from gyroscope and that from accelerometer sensors was used as an input to a Kalman filter to obtain a better tilt estimate. The estimate was then combined with the rotation around the vertical axis to produce a better orientation estimate. However, the estimation was accurate for only brief periods when the subject was not moving and when the acceleration measurements were only due to gravity. Luinge *et al.* developed a method that used constraints in the elbow to measure the orientation of the forearm with respect to the upper arm [4]. They reported an average orientation error of 20°. Giansanti *et al.* combined gyroscopes with accelerometers to track position and orientation during three tasks; stand-to-sit, sit-to-stand and gait-initiation [5]. Estimation error was minimal, however they restricted the application to short periods of 4 s.

Fig. 1. Example of an Opal inertial sensor (APDM, Inc.).

Bachmann *et al.* investigated the effect of electrical and ferromagnetic materials on the accuracy of orientation tracking using a triaxial accelerometer, gyroscope and magnetometer sensors [6]. They observed errors that ranged from 12° to 16° and stated that these errors can be avoided by maintaining an approximate distance of two feet from any source of disturbance. This restricts the use of their tracking system to custom laboratory environment. Yun *et al.* used a quaternion-based EKF to track human body motion. A rotary tilt table with two DOF's was used to assess the performance

M. El-Gohary and J. McNames (Director) are with the Biomedical Signal Processing Laboartory in the Department of Electrical and Computer Engineering at Portland State University (PSU), Portland, Oregon. Email: mahmoud@pdx.edu, mcnames@pdx.edu.

L. Holmstrom is Chief Information Officer at APDM, Inc. Email: lars@apdm.com.

J. Huisinga, E. King, and F. Horak (Director) are members of the Balance Disorders Laboratory in the Department of Neurology at Oregon Health & Science University (OHSU). Email:huisinga@ohsu.edu, kinged@ohsu.edu, horakf@ohsu.edu.

J. McNames, L. Holmstrom, F. Horak, OHSU, and PSU have a significant financial interest in APDM, a company that may have a commercial interest in the results of this research and technology. The potential individual and institutional conflicts of interest have been reviewed and managed by OHSU and PSU.

978-1-4244-4122-8/11/$26.00 ©2011 IEEE

of the tracker [7]. The error for the pitch angle was not reported, and an error of 9° in less than 2 s was obtained for the roll angle. Zhou *et al.* successfully estimated elbow orientation using inertial sensors mounted on the wrist and elbow joints. They integrated the rotational rate to localize the wrist and elbow, and smoothed the abrupt amplitude changes to reduce overshoots of the inertial measurement due fast movements to reduce error in position estimation. They attained a high correlation between position estimates from the inertial tracker and estimates from a reference optical tracking system, ≥ 0.91. However, all the reported correlations were not statistically significant [8].

In this paper we combine kinematic models designed for control of robotic arms with state space methods to directly estimate human joint angles of a multi-segment limb. Estimated joint angles are computed from measured inertial data as a function of time in a single step using a nonlinear state space estimator. The estimator utilizes the unscented Kalman filter which incorporates state space evolution equations based on a kinematic model of the multi-segment limb. The proposed algorithm can be applied to any combination of sensors to track any limb movement in either real-time or off-line processing mode with higher accuracy for slow and fast motion with a minimal number of sensors.

II. Theory

In the analysis and control of robotic manipulators, a robot arm is normally represented as a sequence of links connected by joints [9]. This convention has also also been successfully applied in addressing human motion and is based upon characterizing the configuration between consecutive links by a transformation matrix. If each pair of consecutive links is related via a matrix, then using the matrix chain-rule multiplication, it is possible to relate any segmental link (e.g., between the wrist and elbow) to another (e.g., between the elbow and shoulder).

To obtain a systematic method for describing position and orientation of each pair of consecutive links, we generate a transformation matrix between the links using the Denavit and Hartenberg (D-H) method, starting with attaching frames or coordinate systems to each link [10]. Each frame $\{X_i, Y_i, Z_i\}$ is then related to the previous one using a 4×4 homogeneous transformation matrix. This matrix depends on four parameters associated with each link. The first parameter is the link length a_i which is the distance from Z_i to Z_{i+1} measured along the X_i axis. The second parameter is the link twist α_i which is the angle from Z_i to Z_{i+1} measured about the X_i axis. The distance from X_{i-1} to X_i measured along the Z_i axis is known as the link offset d_i. The fourth parameter is the joint angle θ_i, which is the angle from X_{i-1} to X_i measured about the Z_i axis.

A. Link Transformations

Four transformations are needed to relate the i^{th} frame to its neighboring $(i-1)^{th}$ frame. First, rotate about X_i an angle α_{i-1} to make the two coordinate systems coincide. Next, translate along X_i a distance a_{i-1} to bring the two origins together. Third, rotate about Z_i an angle θ_i to align X_i and X_{i-1}. Finally, translate along Z_i a distance d_{i-1} to bring X_i and X_{i-1} into coincidence. Each of these four operations can be expressed by a basic homogeneous rotation-translation matrix and the product of these four transformation matrices yields a composite matrix ${}^{i-1}_{i}T$, known as the D-H transformation matrix which defines frame i to its adjacent $i-1$

$$
{}^{i-1}_{i}T = \begin{bmatrix} c(\theta_i) & -s(\theta_i) & 0 & a_{i-1} \\ s(\theta_i)c(\alpha_{i-1}) & c(\theta_i)c(\alpha_{i-1}) & -s(\alpha_{i-1}) & -s(\alpha_{i-1})d_i \\ s(\theta_i)s(\alpha_{i-1}) & c(\theta_i)s(\alpha_{i-1}) & c(\alpha_{i-1}) & c(\alpha_{i-1})d_i \\ 0 & 0 & 0 & 1 \end{bmatrix}
$$

where $s(\alpha_{i-1}) = \sin(\alpha_{i-1})$, $c(\theta_i) = \cos(\theta_i)$, etc.

B. Shoulder and elbow joint angle tracker example

As an example, we present a model for forearm movement with shoulder and elbow joints. Fig. 2 shows the base reference frame 0 at the center of the shoulder joint. Frames 1 through 3 represent shoulder flexion/extension, abduction/adduction and internal/external rotation, respectively. Frames 4 through 5 represent the elbow flexion/extension and pronation/supination of the forearm. The two inertial sensors are placed near the wrist and on the upper arm between the shoulder and elbow as shown in Fig. 3. Table I shows the

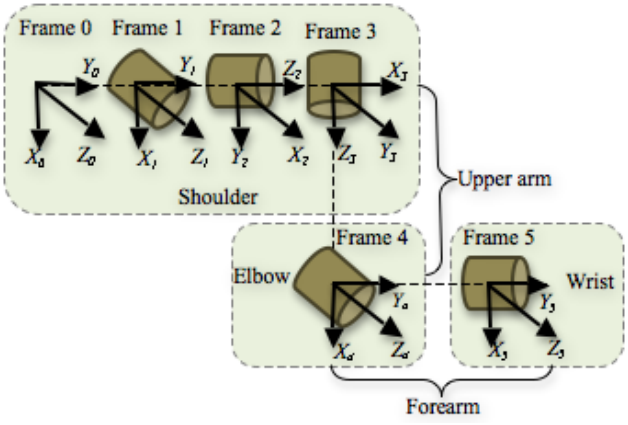

Fig. 2. Kinematics diagram of the arm model with Frame 0 as the reference fame. Frames 1 through 3 represent shoulder flexion/extension, abduction/adduction and internal/external rotation, respectively. Frames 4 through 5 represent the elbow flexion/extension and pronation/supination.

D-H parameters, where α_{i-1} is the angle to rotate to make the two coordinate systems coincide, the length of the upper arm l_{u}, is the distance from Z_3 to Z_4 along the X_4 axis, l_{f} is the length of the forearm, and θ_i is the i^{th} angle of rotation.

C. Velocity and acceleration propagation from link to link

At any instant, each link of the arm in motion has some linear and angular velocity. The linear velocity is that of the origin of the frame. The angular velocity describes the rotational motion of the link. The velocity of link $i+1$ is

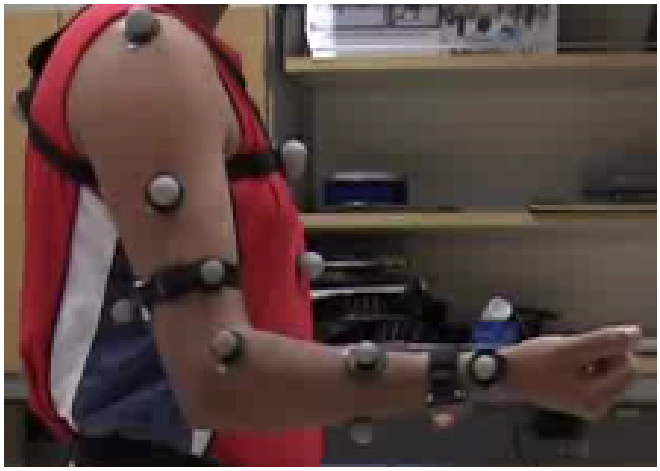

Fig. 3. Subject performing elbow flexion, with one inertial sensor attached with a black band on the wrist and another on the upper arm. Ten reflective markers were attached to the arm, and three were attached to the sternum.

TABLE I

DENAVIT-HARTENBERG PARAMETERS FOR THE ARM MODEL.

Frame	α_{i-1}	a_{i-1}	d_i	θ_i
1	0	0	0	θ_1
2	$-\frac{\pi}{2}$	0	0	θ_2
3	$-\frac{\pi}{2}$	0	0	θ_3
4	$\frac{\pi}{2}$	l_{u}	0	θ_4
5	$-\frac{\pi}{2}$	0	l_{f}	θ_5

that of link i plus the new velocity component added by joint $i+1$

$$ {}^{i}\omega_{i+1} = {}^{i}\omega_i + {}^{i}_{i+1}R\,\dot{\theta}_{i+1}\,{}^{i+1}Z_i, \tag{1} $$

where ${}^{i}_{i+1}R$ is the rotation matrix that relates frame i to frame $i+1$, and is use to represent added rotational components due to motion at the joint in frame i. If we multiply both sides of the equation by ${}^{i+1}_{i}R$, we find the description of the angular velocity of link $i+1$ with respect to frame i+1

$$ {}^{i+1}\omega_{i+1} = {}^{i+1}_{i}R\,{}^{i}\omega_i + \dot{\theta}_{i+1}\,{}^{i+1}Z_{i+1} $$

The linear velocity of the origin of frame $i+1$ is the same as that of the origin of frame i plus a new component caused by the rotational velocity of link i

$$ {}^{i+1}v_{i+1} = {}^{i+1}_{i}R({}^{i}v_i + {}^{i}\omega_i \times {}^{i}P_{i+1}) $$

where ${}^{i}P_{i+1}$ is the position vector of the frame $i+1$ and is the upper right 3×1 vector of the D-H matrix. The angular acceleration from one link to the next is

$$ {}^{i+1}\dot{\omega}_{i+1} = {}^{i+1}_{i}R\,{}^{i}\dot{\omega}_i + {}^{i+1}_{i}R\,{}^{i}\omega_i \times \dot{\theta}_{i+1}\,{}^{i+1}Z_{i+1} + \ddot{\theta}_{i+1}\,{}^{i+1}Z_{i+1} $$

The linear acceleration of each link frame origin is

$$ {}^{i+1}\dot{v}_{i+1} = {}^{i+1}_{i}R\left[{}^{i}\dot{\omega}_i \times {}^{i}P_{i+1} + {}^{i}\omega_i \times ({}^{i}\omega_i \times {}^{i}P_{i+1}) + {}^{i}\dot{v}_i\right] $$

where the single and double dot notation is used to represent first and second derivatives with respect to time. The rotation matrices R can be obtained by taking the transpose of the upper left 3×3 D-H transformation matrix, and the D-H parameters shown in Table I. We initialize $\omega_0 = \dot{\omega}_0 = (0,0,0)^T$, and $\dot{v}_0 = (g_x, g_y, g_z)^T$, where g is gravity. These equations are part of what is known as Newton-Euler equations of motion. The are forward recursive equations that propagate linear and angular velocity and acceleration from the reference coordinate system to the last link.

D. State Space Model

Having defined the kinematic model of the arm, we now formulate the relationship between the measured data and the biomechanical states using a state space model. The general discrete time statistical state-space model is of the form,

$$ x(n+1) = f_n\left[x(n), u(n)\right] \tag{2} $$

$$ y(n) = h_n\left[x(n), v(n)\right] \tag{3} $$

where n is the discrete time index, $x(n)$ is the unobserved state of the system, $y(n)$ is the observed or measured data, $f_n[\cdot]$ and $h_n[\cdot]$ are nonlinear state and observation equations, $u(n)$ is process noise, and $v(n)$ is an observation noise. Both $u(n)$ and $v(n)$ are assumed to be white noise processes with zero mean. The state model equations which describe the evolution of the states with time are given by

$$ \theta_i(n+1) = \theta_i(n) + T_{\mathrm{s}}\dot{\theta}_i(n) + \frac{1}{2}T_{\mathrm{s}}^2\ddot{\theta}_i(n) \tag{4} $$

$$ \dot{\theta}_i(n+1) = \dot{\theta}_i(n) + T_{\mathrm{s}}\ddot{\theta}_i(n) \tag{5} $$

$$ \ddot{\theta}_i(n+1) = \alpha\ddot{\theta}_i(n) + u_{\ddot{\theta}_i}(n) \tag{6} $$

where $i = \{1,\ldots,5\}$, $\theta_i(n)$ is the i^{th} angle at time n, $\dot{\theta}_i(n)$ is the angular velocity of the i^{th} angle at time n, $\ddot{\theta}_i(n)$ is the angular acceleration of the i^{th} angle at time n, $u_{\ddot{\theta}_i}(n)$ is a white noise process with zero mean, α is a process model parameter, and $T_{\mathrm{s}} = 1/f_{\mathrm{s}}$ is the sampling period. These are standard equations for a physical object traveling at a constant acceleration. In this case the model assumes the acceleration is constant for the duration of a sampling interval, which is short enough (approximately 8 ms) for this approximation to be sufficiently accurate for tracking. The model of angular acceleration is a first-order autoregressive process with zero mean. Typically the value of α will be assigned an intermediate value that represents typical patterns of human motion in joint angles.

The observation model describes the relationship of the states to the observed data obtained from the inertial sensor. We assume that the inertial sensor includes triaxial accelerometers and triaxial gyroscopes. This simple model assumes the sensor noise is additive and white, but could be easily generalized to include drift, which is common to MEMS inertial sensors.

$$ y(n) = \begin{bmatrix} \omega_x(n) \\ \omega_y(n) \\ \omega_z(n) \\ \dot{v}_x(n) \\ \dot{v}_y(n) \\ \dot{v}_z(n) \end{bmatrix} + \begin{bmatrix} v_{gx}(n) \\ v_{gy}(n) \\ v_{gz}(n) \\ v_{ax}(n) \\ v_{ay}(n) \\ v_{az}(n) \end{bmatrix}, \tag{7} $$

where ω_x, ω_y and ω_z are the angular velocities along the x, y and z axes, respectively. The gyroscope noise along the

different axes is described by v_{gx}, v_{gy} and v_{gz}. Similarly, the translational accelerations along the three axes are $\dot{v}_x$, $\dot{v}_y$ and $\dot{v}_z$, and the accelerometer noise is given by v_{ax}, v_{ay} and v_{az}. The acceleration measurement vector includes translational accelerations and the effects of gravity.

E. Nonlinear state estimator

The arm model introduced above exhibits nonlinearities. The use of the linear Kalman filter in a highly nonlinear dynamics introduces estimation errors. The most common approach to solving the nonlinear estimation problem is the extended Kalman filter (EKF), which is based upon linearizing the state and observation models with a first-order Taylor expansion. However, this linearization leads to poor performance if the dynamics are highly nonlinear and the simple linearized model based on the gradient is an inaccurate approximation. The EKF also requires Jacobian matrices and inverse matrix calculation. Alternatively, sequential Monte Carlo methods (i.e, particle filters), which are applicable to highly nonlinear and non-Gaussian estimation problems, allow for a complete representation of the density function of the unobserved states using a finite number of samples. However, particle filters require much more computation. The unscented Kalman filter (UKF) has nearly the same computational requirements as the EKF, but uses a more accurate method to characterize the nonlinear effects. The results in this paper were generated with a UKF [11].

III. Results

To evaluate the performance of the inertial tracking system in monitoring arm movement, the joint angles calculated by the inertial tracker were compared to those obtained by an optical tracking system, used as a reference system. The study was conducted in the Balance Disorders Laboratory at OHSU, which is equipped with an optical motion tracking system that comprises eight high-speed, infrared cameras (Eagle Analog System, Motion Analysis Corporation, California). The cameras record position of reflective markers placed on the upper arm, forearm, shoulder and wrist. Optical relative joint angles were calculated from three-dimensional markers positions using Grood's method [12]. One subject performed a set of tasks described in Table II. Each articulation was performed for 15 s while keeping the rest of the body still. The correlation coefficients between the angle estimates from the inertial tracker and estimates from the reference optical tracking system were all statistically significant ($p < .05$) and ≥ 0.91.

TABLE II

Correlation between optical and inertial angles of shoulder and elbow of a subject performing a set arm movement.

Task	R (normal speed)	R (fast speed)
Elbow Flexion/Extension	0.92	0.89
Elbow Supination/Pronation	0.96	0.93
Shoulder Flexion/Extension	0.97	0.94
Shoulder Abduction/Adduction	0.94	0.91

One of the limitations of previous tracking methods is that they performed well only during slow movements. To determine the capability of the proposed algorithm of tracking fast activities, the subject was instructed to repeat the same activities as fast as they could. On average, the subject reached from initial anatomical position to maximum joint movement range in 0.5 s, compared to 1.0 s during normal speed activities. Although, the correlation was slightly lower than that for the regular speed, the correlation coefficients were still statistically significant ($p < .05$) and were all ≥ 0.89.

IV. Conclusion

This paper described a new method for estimating joint angles of a multi-segment limb using inertial sensors. Estimated joint angles are computed from measured inertial data as a function of time in a single step using a nonlinear state space estimator. The estimator utilizes the unscented Kalman filter which incorporates state space evolution equations based on a kinematic model of the multi-segment limb. The algorithms outlined in this paper can be applied to any combination of sensors, and could be generalized to track any limb movement in either real-time or off-line with higher accuracy for slow and fast motion with a minimal number of sensors.

References

[1] O. Woodman, "An introduction to inertial navigation," Computer Laboratory, University of Cambridge, UK, Tech. Rep., August 2007.

[2] D. Roetenberg, "Inertial and magnetic sensing of human motion," Ph.D. dissertation, University of Twente, Enschede, The Netherlands, 2006.

[3] H. J. Luinge, "Inertial sensing of human motion," Ph.D. dissertation, Univeristy of Twente, Enschede, The Netherlands, December 2002.

[4] H. J. Luinge, P. H. Veltink, and C. T. M. Baten, "Ambulatory measurement of arm orientation," *Journal of Biomechanics*, vol. 40, pp. 78–85, 2007.

[5] D. Giansanti, G. Maccioni, and V. Macellari, "The development and test of a device for the reconstruction of 3-d position and orientation by means of a kinematic sensor assembly with rate gyroscopes and accelerometers," *IEEE Transactions on Biomedical Engineering*, vol. 52, no. 7, pp. 1271–1277, 2005.

[6] E. R. Bachmann, X. Yun, and C. Peterson, "An investigation of the effects of magnetic variations on inertialklagnetic orientation sensors," in *Proceedings of the 2004 IEEE International Conference on Robotics and Automation*, 2004, pp. 1115–1122.

[7] X. Yun and E. R. Bachmann, "Design, implementation, and experimental results of a quaternion-based kalman filter for human body motion tracking," *IEEE Transaction on Robotics*, vol. 22, pp. 1217–1227, 2006.

[8] H. Zhou and H. Hu, "Upper limb motion estimation from inertial measurements," *International Journal of Information Technology*, vol. 13, no. 1, pp. 1–14, 2007.

[9] J. J. Craig, *Introduction to Robotics, Mechanics and Control*, ser. Electrical and Computer Engineering: Control Engineering. Addison-Wesley, 1989.

[10] J. Denavit and R. S. Hartenberg, "A kinematic notation for lower-pair mechanisms based on matrices," *Applied Mechanics.*, vol. 23, pp. 215–221, 1955.

[11] S. J. Julier and J. K. Uhlmann, "Unscented filtering and nonlinear estimation," in *Processings of The IEEE*, vol. 92, March 2004, pp. 401–422.

[12] E. S. Grood and W. J. Suntay, "A joint coordinate system for the clinical description of three-dimensional motions: Application to the knee," *ASME*, vol. 105, pp. 136–142, 1983.